Implementation of Convolutional Perfectly Matched Layer Absorbing Boundary Condition with FDTD Method

Abdul Aleem Jamali†, Kelash Kanwar†, Majid Hussain†, Kamran Ali Memon†,†† and Fareed Ahmed Jokhio†††

†Department of Electronic Engineering, Quaid-e-Awam University of Engineering, Science and Technology, Nawabshah, Pakistan
††School of Electronic Engineering, Beijing University of Posts and Telecommunications (BUPT), Xitucheng Road No. 10, Beijing, China 100876
†††Department of Computer Engineering, Quaid-e-Awam University of Engineering, Science and Technology, Nawabshah, Pakistan

Summary
Restricting the size of computational domain in the simulation is highly important to save computational resources. Absorbing boundary conditions (ABCs) are used for limiting the computational area together with other boundary conditions (i.e. Dirichlet or Neumann boundary conditions). ABCs such as Perfectly Matched Layers (PMLs) are implemented for the analysis of electromagnetic problems such scattering, photonic crystals, and radiation. The objective of this paper is to present the efficient implementation of ABCs by using Finite Difference Time Domain (FDTD) algorithm. In comparison to other numerical algorithms, FDTD technique offers high level performance in a single simulation run, even if the problem area and range of frequencies increased. This paper shows the implementation of Convolutional Perfectly Matched Layer (CPML) absorbing boundary condition instead of PML by preparing CPML code in FDTD algorithm. It is demonstrated from the computational results that CPML is more efficient in terms of performance of absorbing electromagnetic waves.

Key words:
Computational Electromagnetics, Absorbing Boundary Conditions, Convolutional Perfectly Matched Layer, Finite Difference Time Domain Method, Numerical Methods.

1. Introduction

In today's computational electromagnetic (CEM) world, the theoretical and technological progress of the computational resources made the finite difference time domain (FDTD) algorithm most admired numerical technique.

FDTD algorithm is used for the design and electromagnetic analysis of antenna, microwave circuits and photonic devices. In the electromagnetic simulation, the computational domain is required to be truncated to simulate infinite space. For this purpose, Absorbing boundary conditions (ABCs) are implemented at the boundaries of the computational domain in FDTD simulations. ABCs are used to absorb electromagnetic waves. The efficient and accurate implementation of the ABCs in FDTD technique is highly challenging task. The simulation of the FDTD lattice needs to be extended to infinity for efficient and accurate implementation of ABCs. The perfectly matched layer (PML) is a famous ABC which can absorb electromagnetic waves of any polarization, incident angle and frequency (or wavelength). It had been proved to be effective for regions of homogeneous, inhomogeneous, dispersive, linear, nonlinear as well as anisotropic media. Berenger [1] in 1994 has introduced the PML which was based on the field-splitting method of unbounded Maxwell's equations in FDTD. It produces sufficient discretization error in the lattices of FDTD. Then, Uniaxial PML (UPML) with anisotropic media (i.e. permittivity tensors) has been proposed in [2]. The UPML was implemented by Gedney [3] in 1996 for the truncation of FDTD lattices. As compared to split-field PML, the discretization error is minimized in UPML while keeping efficiency same [4]. After the recognition of the concept of PML, different modifications in the PML [5] have been proposed such as stretched coordinate (SC), complex frequency shifted (CFS), recursive convolution and Convolutional PML (CPML) formulation for the absorption of electromagnetic waves. The SC PML formulation has broadened the utilization of PML into general curvilinear [6] as well in orthogonal [7] coordinate systems. The PML based SC formulation has the disadvantage of being weak causal. The causality of PML has been improved by using CFS tensor coefficients based formulation [8]. Roden and Gedney have proposed CPML for arbitrary media [9]. It is independent of the primary medium and it does not require any modification when applying in arbitrary media such as lossless, lossy, inhomogeneous, nonlinear, anisotropic and dispersive media. It has higher performance as compared

Manuscript received December 5, 2018
Manuscript revised December 20, 2018

to other PMLs. Recently, several improvements in the CPMLs have been demonstrated [10, 11].
In this paper, CPML is implemented by using FDTD algorithm for 2-dimensional (2D) case. The CPML ABC is defined at the top and bottom layer of the computational domain. CPML coefficients and parameters are computed for the efficient implementation. Section-1 gives the brief introduction and literature review of PMLs. Section-2 provides the details of the implementation of the FDTD method. Results are demonstrated and discussed in Section-3. Finally, Section-4 concludes the outlined research work.

2. Implementation

In order to implement the CPML boundary conditions by using FDTD method. Out of four Maxwell's equation, the two unbounded equations of differential form are utilized in FDTD. The one Maxwell's equation describes the Faraday's law of electromagnetic induction, and the other equation defines the Ampere's law together with continuity equation. Yee's [12] has developed a technique which is used for discretization of the differential form of Maxwell's equations. In this technique, two cubic lattices are introduced which are orthogonal to each other. The Computational domain is made up of those orthogonal cubic lattices. The one cube is called primary and the other cubic lattice which is orthogonal to first one is called secondary cubic lattice. The electric field components are spatially placed at the primary cubic lattice, while magnetic field components are sampled at the corners of secondary cubic lattice. Since, both the cubic lattices are orthogonal to each other; the electric and magnetic field components would encircle each other in spatial domain. For differential time domain, electric and magnetic field are discretized at half time space from each other. For a 2D simulation, either transverse electric (TE) or transverse magnetic (TM) mode is selected. Here, TM mode is chosen; which is constituted of Hx, Ey and Hz components. The updating 2D Maxwell's equations are given by Eq. (1) to Eq. (3) [12],

$$H_x^{(n_x,n_z,n_t)} = H_x^{(n_x,n_z,n_t-1)} + \frac{\Delta t}{\mu_0}\left[\frac{E_y^{(n_x,n_z+1/2,n_t-1/2)} - E_y^{(n_x,n_z-1/2,n_t-1/2)}}{\Delta z}\right], \qquad (1)$$

$$E_y^{(n_x+1/2,n_z+1/2,n_t+1/2)} = E_y^{(n_x+1/2,n_z+1/2,n_t-1/2)} - \frac{\Delta t}{\epsilon_0}\left[\frac{H_x^{(n_x,n_z+1,n_t)} - H_x^{(n_x,n_z,n_t)}}{\Delta z} - \frac{H_z^{(n_x+1,n_z,n_t)} - H_z^{(n_x,n_z,n_t)}}{\Delta x}\right] \qquad (2)$$

$$H_z^{(n_x,n_z,n_t)} = H_z^{(n_x,n_z,n_t-1)} - \frac{\Delta t}{\mu_0}\left[\frac{E_y^{(n_x+1/2,n_z,n_t-1/2)} - E_y^{(n_x-1/2,n_z,n_t-1/2)}}{\Delta x}\right] \qquad (3)$$

The time-stepping process defined in the FDTD algorithm is entirely explicit; therefore there is no need to do inversion of matrix. This property of the FDTD makes it to be implemented easily [13]. For the numerical stability of the simulation in FDTD method, the time step Δt is required to be smaller than the differential size (Δs) of the lattice in space. The differential time of Δt= Δs/c0 is needed to be propagated at a distance of single cubic cell [13]. The numerical stability in FDTD can be achieved by satisfying the Courant condition i.e. Δt= Δs/√n c, where n and c are simulation dimension and the speed of light in vacuum, respectively [14].
For the implementation of ABC, a novel method known as CPML is introduced by J. Alen Roden and Stephen Gedney in the paper [9]. The time dependent form of the Maxwell's equations in the stretched space coordinate is the basis for the CPML. For a 2-D TMy case, the CPML region is updated by the following equations (Eq. 4 to Eq. 6) [11, 14].

$$H_x^{(n_x,n_z,n_t)} = H_x^{(n_x,n_z,n_t-1)} + \frac{\Delta t}{\mu_0}\left[\frac{E_y^{(n_x,n_z+1/2,n_t-1/2)} - E_y^{(n_x,n_z-1/2,n_t-1/2)}}{k_{mz}\Delta z} + \psi_{m_{xz}}^{(n_x,n_z,n_t-1/2)}\right] \qquad (4)$$

$$H_z^{(n_x,n_z,n_t)} = H_z^{(n_x,n_z,n_t-1)} - \frac{\Delta t}{\mu_0}\left[\frac{E_y^{(n_x+1/2,n_z,n_t-1/2)} - E_y^{(n_x-1/2,n_z,n_t-1/2)}}{k_{mx}\Delta x} - \psi_{m_{zx}}^{(n_x,n_z,n_t-1/2)}\right] \qquad (5)$$

$$E_y^{(n_x+1/2,n_z+1/2,n_t+1/2)} = E_y^{(n_x+1/2,n_z+1/2,n_t-1/2)} - \frac{\Delta t}{\varepsilon_0}\left[\frac{H_x^{(n_x,n_z+1,n_t)}-H_x^{(n_x,n_z,n_t)}}{k_{ez}\Delta z} - \frac{H_z^{(n_x+1,n_z,n_t)}-H_z^{(n_x,n_z,n_t)}}{k_{ex}\Delta x} + \psi_{e_{yz}}^{(n_x+1/2,n_z+1/2,n_t)} - \psi_{e_{yx}}^{(n_x+1/2,n_z+1/2,n_t)}\right] \quad (6)$$

where $\psi_{m_{xz}}^{(n_x,n_z,n_t-1/2)}$, $\psi_{m_{zx}}^{(n_x,n_z,n_t-1/2)}$, $\psi_{e_{yz}}^{(n_x+1/2,n_z+1/2,n_t)}$, $\psi_{e_{yx}}^{(n_x+1/2,n_z+1/2,n_t)}$ are auxiliary expressions and are updated using Eq. (7) to Eq. (24).

$$\psi_{m_{xz}}^{(n_x,n_z,n_t-1/2)} = b_{mz}\psi_{m_{xz}}^{(n_x,n_z,n_t-1)} + a_{mz}\left[\frac{E_y^{(n_x,n_z+1/2,n_t-1/2)}-E_y^{(n_x,n_z-1/2,n_t-1/2)}}{\Delta z}\right] \quad (7)$$

$$\psi_{m_{zx}}^{(n_x,n_z,n_t-1/2)} = b_{mx}\psi_{m_{xz}}^{(n_x,n_z,n_t-1)} + a_{mx}\left[\frac{E_y^{(n_x+1/2,n_z,n_t-1/2)}-E_y^{(n_x-1/2,n_z,n_t-1/2)}}{\Delta x}\right] \quad (8)$$

$$\psi_{e_{yz}}^{(n_x+1/2,n_z+1/2,n_t)} = b_{ez}\psi_{e_{yz}}^{(n_x,n_z,n_t-1)} + a_{ez}\left[\frac{H_x^{(n_x,n_z+1,n_t)}-H_x^{(n_x,n_z-1,n_t)}}{\Delta z}\right] \quad (9)$$

$$\psi_{e_{yx}}^{(n_x+1/2,n_z+1/2,n_t)} = b_{ex}\psi_{e_{yx}}^{(n_x,n_z,n_t-1)} + a_{ex}\left[\frac{H_z^{(n_x+1,n_z,n_t)}-H_z^{(n_x-1,n_z,n_t)}}{\Delta x}\right] \quad (10)$$

Where, the coefficients α_{mz}, α_{mx}, α_{ez}, α_{ex}, b_{mz}, b_{mx}, b_{ez}, and b_{ex} are computed by Eq. (11) to Eq. (18) [15].

$$a_{mz} = \frac{\sigma_{mz}}{(\sigma_{mz}k_{mz}+k_{mz}^2\alpha_{mz})}(b_{mz}-1.0), \quad (11)$$

$$a_{mx} = \frac{\sigma_{mx}}{(\sigma_{mx}k_{mx}+k_{mx}^2\alpha_{mx})}(b_{mx}-1.0), \quad (12)$$

$$a_{ez} = \frac{\sigma_{ez}}{(\sigma_{ez}k_{ez}+k_{ez}^2\alpha_{ez})}(b_{ez}-1.0), \quad (13)$$

$$a_{ex} = \frac{\sigma_{ex}}{(\sigma_{ex}k_{ex}+k_{ex}^2\alpha_{ex})}(b_{ex}-1.0), \quad (14)$$

$$b_{mz} = e^{\left(-\left(\sigma_{mz}/k_{mz}\right)+(\alpha_{mz})\right)\Delta t/\mu_0}, \quad (15)$$

$$b_{mx} = e^{\left(-\left(\sigma_{mx}/k_{mx}\right)+(\alpha_{mx})\right)\Delta t/\mu_0}, \quad (16)$$

$$b_{ez} = e^{\left(-\left(\sigma_{ez}/k_{ez}\right)+(\alpha_{ez})\right)\Delta t/\varepsilon_0}, \quad (17)$$

$$b_{ex} = e^{\left(-\left(\sigma_{ex}/k_{ex}\right)+(\alpha_{ex})\right)\Delta t/\varepsilon_0}. \quad (18)$$

In this technique, PML is started with the zero conductivity at the interface and the value of the conductivity is increased gradually as the depth of the PML is increased. For example, a polynomial distribution is used to set up the conductivity (Eq. (19)) taken from [9],

$$\sigma^e(z) = (z/l)^m\,\sigma^e_{max}. \quad (19)$$

The value of the conductivity increases from 0 at the interface (z = 0) to σ^e_{max} at the truncation boundary (z = *l*). Hence, both finite thickness truncation error and discontinuous conductivity error can be suppressed to a desired level [11, 15].

By setting $\varepsilon = \varepsilon_0$ and $\mu = \mu_0$, and enforcing the following condition given in Eq. (20).

$$\frac{\sigma^m}{\mu} = \frac{\sigma^e}{\varepsilon}, \quad (20)$$

With $\eta_0 = \eta_1$ and the reflection coefficient $\Gamma = 0$. There is no reflection coming from the interface, therefore region 1 and region 2 are perfectly matched for incident condition as shown in Fig. 1.

In order to reduce discretization error k_z must be scaled between 1 and k_z^{max} (Eq. (21)) such that it is 1 at the front boundary and k_z^{max} at the PEC wall (see Fig. 1) [16, 17]. For a PML of depth d with boundary interface z = 0, hence

$$k_z(z) = 1 + (k_{max}-1)\left(\frac{z}{d}\right)^m, \quad (21)$$

It is required to scale α_z such that it is maximum at the interface and minimum at the back wall [15]. The two different recommended polynomial scaling are [16] given by Eq. (22).

$$\alpha_z(z) = \alpha_z^{max}\left(1-\left(\frac{z}{d}\right)^m\right),\ \alpha_z(z) = \alpha_z^{max}\left(\left(1-\frac{z}{d}\right)^m\right). \quad (22)$$

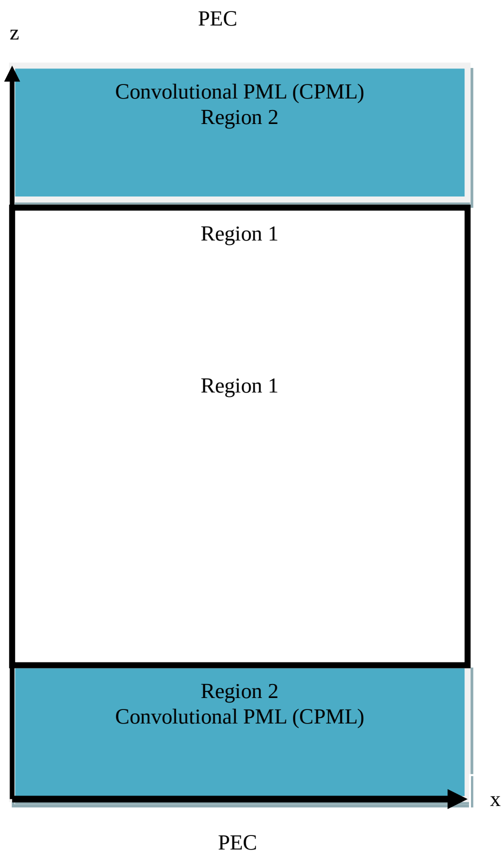

Fig. 1 Convolutional Perfectly Matched Layer (i.e. CPML) absorbing boundary condition at the top and bottom of the computational domain along the z-direction

3. Results and Discussion

For the computation of the CPML, consider the FDTD model as shown in Fig. 1, where CPML is implemented at the top and bottom of the computational domain in the vertical directions (along z-direction).

In order to implement the CPML in the time-marching scheme, coefficients and auxiliary parameters are required to be defined and initialized before the start of loop for time marching [18]. Before assigning arrays, the size of the computational domain must be computed by taking into account the thickness of CPML [18]. In this case, the problem space consists of 260 cells in the x-direction and 260 cells in the z-direction which includes 10 cells up and down for CPML region. After the CPML the boundaries are considered to be PEC, the CPML parameters $\sigma^e(z),\ \sigma^m(z), k^e(z),\ k^m(z),\ \alpha^e(z),\ \alpha^m(z)$ are distributed towards the thickness of CPML in one-dimensional array. The CPML parameters are used to update electric and magnetic field components. Positions of the field components and the distances from the CPML interface are considered to be compensated from the first CPML cell by half cell size. The coefficients αmz, αmx, αez, αex, bmz, bmx, bez, and bex are also one-dimensional functions of the depth of the CPML. The distribution of the CPML parameters and the coefficients in the bottom and top layers are shown in Fig. 3 and Fig. 4, respectively. The CPML parameters are calculated by Eq. (23) to Eq. (28).

$$\sigma^e(z) = \left(\frac{(z-0.5*\Delta z)}{d}\right)^m \sigma_{max}, \quad (23)$$

$$\sigma^m(z) = \left(\frac{\mu_0}{\varepsilon_0}\right)\left(\frac{z}{d}\right)^m \sigma_{max}, \quad (24)$$

$$k^e(z) = 1 + (k_{max} - 1)\left(\frac{(z-0.5*\Delta z)}{d}\right)^m, \quad (25)$$

$$k^m(z) = 1 + (k_{max} - 1)\left(\frac{z}{d}\right)^m, \quad (26)$$

$$\alpha^e(z) = \alpha_z^{max}\left(1 - \left(\frac{(z-0.5*\Delta z)}{d}\right)^m\right). \quad (27)$$

$$\alpha^m(z) = \left(\frac{\mu_0}{\varepsilon_0}\right)\left(1 - \left(\frac{z}{d}\right)^m\right)\alpha^{max}. \quad (28)$$

For this example, the values of $\alpha^{max}, k_{max}, \sigma_{max}$ are [18]: $\alpha^{max} = 0.025$, $k_{max} = 7$, $\sigma_{max} = 1.1\sigma_{opt}$, and $\sigma_{opt} = \frac{m+1}{150\pi\sqrt{\varepsilon_r}\,\Delta z}$. Where, m is the order of the polynomial scaling and is equal to $m = 4$ and $\varepsilon_r = 1$. The updating equations for auxiliary parameters and electric and magnetic field components are implemented by using Eq. (4) to Eq. (10).

The bottom and top CPML is comprised of 10 cells each starting from cell 1 to cell 10 along vertical direction i.e. y-direction (see Fig. 1). For bottom CPML, cell 10 is at the interface between Region 1 and Region 2, while the cell 1 is at the interface between region 2 and PEC, as shown in Fig. 2. For top CPML, cell 1 is at the interface between Region 1 and Region 2, while the cell 10 is at the interface between region 2 and PEC, as shown in Fig. 3. The value of conductivity (sigma) is zero at the interface between Region 1 and Region 2 and is gradually increasing with depth of the CPML reached to a maximum value at the PEC boundary. The value of kappa (k) is 1 at the interface between Region 1/Region 2 and is scaled to maximum at a PEC wall. The value of alpha (αz) is maximum at the interface of Region1/Region2 and is decreasing with depth of CPML reaches to a minimum value at the PEC boundary. Hence, both finite thickness truncation error and discontinuous conductivity error are suppressed.

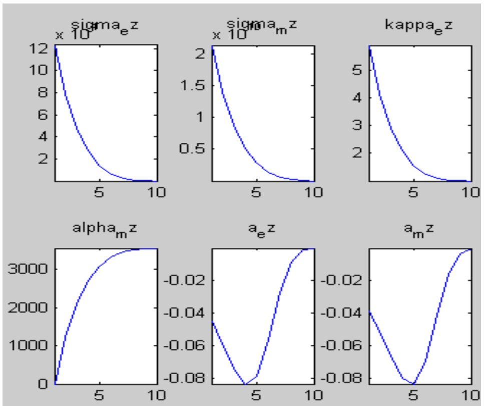

(a)

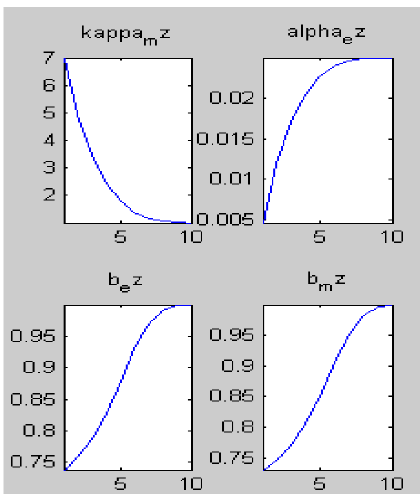

(b)

Fig. 2 The distribution of CPML parameters and coefficients in the bottom layer as a function of depth (horizontally).

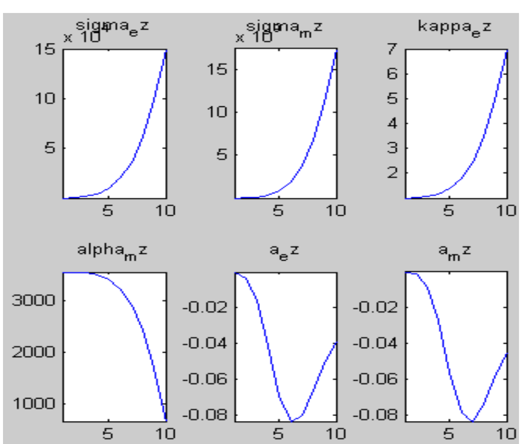

(a)

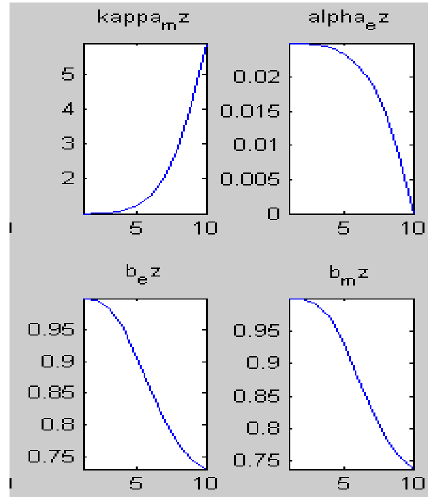

(b)

Fig. 3 The distribution of CPML parameters and coefficients in the top layer as a function of depth (horizontally).

4. Conclusions

The CPML ABC is implemented by using FDTD method. The 2D computational domain is modeled in FDTD for the computation of boundary conditions. The CPML boundary conditions are implemented on the top and bottom side of the computational domain. CPML boundary conditions are used as absorbing boundary conditions. The CPML parameters and coefficients are computed. The results of CPML have shown that it has negligible reflection together with finite thickness truncation error and discontinuous conductivity errors. The CPML is proved to be an efficient boundary condition for the absorption of electromagnetic waves.

References

[1] J. P. Berenger, “A Perfectly Matched Layer for the Absorption of Electromagnetic Waves”, Journal of Computational Physics, vol.114, pp.185–200, 1994.
[2] Z. S. Sacks, D. M. Kingsland, R. Lee and J. F. Lee, “A Perfectly Matched Anisotropic Absorber for Use as an Absorbing Boundary Condition”, IEEE Trans. Antennas Propagat., vol. 43, 1460–1463, 1995.
[3] S. D. Gedney, “An Anisotropic Perfectly Matched Layer Absorbing Media for the Truncation of FDTD Lattices”, IEEE Trans. Antennas Propagat., vol. 44, 1630–1639, 1996.
[4] B. Gvozdic, D. Durdevic and N. Raicevic, “CPML Parameter Optimization in FDTD Modeling of Impulse Source”, The Facta Universitatis, Series: Automatic Control and Robotics (FU Aut Cont Rob), vol. 16(3), 229–240, 2017.
[5] S. D. Gedney, G. Liu, J.A. ROden and A. Zhu, “Perfectly Matched Layer Media with CFS for an Unconditionally

Stable ADI-FDTD Method", IEEE Trans. Antennas Propagat., vol. 49(11), 1554–1559, 2001.
[6] N. V. Kantartzis and T.D. Tsiboukis, "A Higher Order Nonstandard FDTD-PML Method for the Advanced Modeling of Complex EMC Poblems in Generalized 3-D Curvilinear Coordinates", IEEE Transactions on Electromagnetic Compatibility, vol. 46(1), 2–11, 2004.
[7] W. C. Chew and W. H. Weedon, "A 3D Perfectly Matched Medium from Modified Maxwell's Equations with Stretched Coordinates", IEEE Microwave Guided Wave Lett., vol. 7, 599–604, 1994.
[8] X. Zhao, Y. Ji, S. Qiu, S. Guan and Y. Wu, "The CFS-PML in Numerical Simulation of ATEM", Proc. SPIE 10322, Seventh International Conference on Electronics and Information Engineering, 103222F, 2017.
[9] J. A. Roden and S. D. Gedney, "Convolutional PML (CPML): An Efficient FDTD Implementation of the CFS-PML for Arbitrary Media", Microwave Optical Tech. Lett., vol. 27, 334–339, 2000.
[10] S. Fang, H. Pan, T. Du, A.A. Konate, C. Deng, Z. Qin, B. Guo, L. Peng, H. Ma, G. Li and F. Zhou, "Crosswell electromagnetic modeling from impulsive source: Optimization strategy for dispersion suppression in convolutional perfectly matched layer", Sci. Rep. 6, 32613, 2016.
[11] B. D. Gvozdic and D. Z. Djurdjevic, "Performance advantages of CPML over UPML absorbing boundary conditions in FDTD algorithm", Journal of Electrical Engineering, vol. 68 (1), pp. 47-53, 2017.
[12] K. S. Yee, "Numerical Solution of Initial Boundary Value Problems Involving Maxwell's Equations in Isotropic Media", IEEE Transaction on Antennas and Propagation, vol. 14, pp. 302-307, May, 1966.
[13] J. E. Diener, J. Quimby, K. A. Remley, and A. Z. Elsherbeni, "Millimeter-wave frequency FDTD simulation for error vector magnitude of modulated signals", International Applied Computational Electromagnetics Society Symposium (ACES), Denver, CO, USA, 25-29 March, 2018.
[14] J. Yu, R. Malekian, J. Chang, and B. Su, "Modeling of Whole-Space Transient Electromagnetic Responses Based on FDTD and its Application in the Mining Industry", IEEE Transactions on Industrial Informatics, vol. 13 (6), pp. 2974-2982, 2017.
[15] M. Dong, J. Chen, and A. Zhang, "A Convolutional Perfectly Matched Layer (CPML) for the Fourth-Order One-Step Leapfrog HIE-FDTD Method", Applied Computational Electromagnetics Society Journal, vol. 33 (1), pp. 1-6, 2018.
[16] H. L. Jiang, J. F. Zhang, W. X. Jiang, and T. J. Cui, "Unconditionally Stable CN-PML Algorithm for Frequency-Dispersive Left-Handed Materials", IEEE Antennas and Wireless Propagation Letters, vol. 16, pp. 2006-2009, 2017.
[17] G. Q. He, J. H. Stiens, W. S., and Bi. Z. Wang, "Recursively Convolutional CFS-PML in 3-D Laguerre-FDTD Scheme for Arbitrary Media", IEEE Transactions on Microwave Theory and Techniques, vol. 66 (5), pp. 2070-2079, 2018.
[18] A. Darvish, B. Zakeri, and N. Radkani, "An Optimized Hybrid Convolutional Perfectly Matched Layer for Efficient Absorption of Electromagnetic Waves", Journal of Computational Physics, vol. 356, pp. 31-45, 2018.

Abdul Aleem Jamali received B.E. degree in Electronic Engineering in 2006 from Mehran University of Engineering and Technology, Jamshoro. After that he pursued for higher qualification to Germany where he received M.Sc. in Electrical and Communication Engineering and Ph.D. degrees from University of Kassel, Germany in 2011 and 2015, respectively. He is currently working as Assistant Professor, Department of Electronic Engineering, Quaid-e-Awam University of Engineering, Science and Technology, Nawabshah. His research interests include Engineering Electromagnetics, Plasmonics, Optoelectronics, and UWB antennas.